Journal of Alloys and Compounds, 190 (1993) 189–195
JALCOM 419

NMR, magnetism and Mössbauer effect in icosahedral $Al_{63}Cu_{24.5}Fe_{12.5}$ – a thermodynamically stable quasi-periodic alloy

A. R. Drews, M. Rubinstein and G. H. Stauss
Materials Physics Branch, Naval Research Laboratory, Washington, DC 20375 (USA)

L. H. Bennett and L. J. Swartzendruber
National Institute of Standards and Technology, Gaithersburg, MD 20899 (USA)

(Received April 17, 1992; in final form July 7, 1992)

Abstract

We report results of ^{27}Al nuclear magnetic resonance (NMR), magnetism and iron-site Mössbauer experiments on the thermodynamically stable and "perfectly" quasicrystalline icosahedral alloy $Al_{63}Cu_{24.5}Fe_{12.5}$. NMR experiments were performed at 11.10, 17.8 and 45.7 MHz and at temperatures as low as 50 K. Magnetization was measured at 295, 100 and 5 K, while iron site Mössbauer was measured at 295 and 4.2 K. We find very small NMR Knight shifts and long relaxation times that we interpret as consistent with a pseudo-gap in the density of states near the Fermi level. NMR line shapes in AlCuFe do not show quadrupolar structure consistent with a single aluminum site. We report results of numerical simulations that effectively reproduce the features and trends in observed line shapes by means of a broad distribution of electric field gradients (EFGs) at aluminum sites. Our magnetization and Mössbauer effect experiments show that there is a very small fraction of the material that is magnetically ordered at low temperatures. This magnetic behavior was only observed well below the lowest temperature of NMR experiments and cannot be responsible for the broad NMR lines. Iron-site Mössbauer lines show significant broadening characteristic of a distribution of EFGs that is qualitatively similar to that indicated for the aluminum site.

1. Introduction

Previous NMR measurements on icosahedral AlMnSi [1], AlMnRuSi [2] and AlCuLi [3] showed very small Knight shifts and smooth spectra without sharp quadrupole structure. The absence of a significant Knight shift can be interpreted as resulting from a low density of electronic states at the Fermi level, while the lack of sharp structure in the line shape was interpreted as the result of a distribution of aluminum site EFGs. Recent studies of transport properties [2–6], NMR [1–3] and magnetization [2] have pointed towards the existence of a pseudo-gap at the Fermi level. This gap has been described in band structure calculations by Fujiwara and Yokokawa [7] for icosahedral AlCuLi and for AlFe. They suggest a universal gap due to critical localization of states near the Fermi level that may be responsible for enhanced cohesive energies necessary for the formation of the icosahedral phase. Interpretation of previous measurements in icosahedral materials was hampered by the fact that many of these materials were not thermodynamically stable and the existence of multiple phases could not be ruled out. Our measurements show that small Knight shifts and a broad distribution of sites in these materials are intrinsic effects and not sensitive to the thermodynamic stability of the alloys.

2. NMR theory

The NMR Hamiltonian for a nuclear spin I in a magnetic field $\boldsymbol{H}$ can be written as

$$H = -\gamma h \boldsymbol{I}\cdot\boldsymbol{H} + \frac{h\nu_Q}{6}\{3I^2_z - I^2 - \eta[I^2_x - I^2_y]\} - \gamma h \boldsymbol{I}\cdot\boldsymbol{K}\cdot\boldsymbol{H} \quad (1)$$

where the first term represents the nuclear Zeeman effect, the second term the quadrupole interaction between the nucleus and the electric field gradient, and the third term represents the interaction between the nucleus and the conduction electrons. In eqn. (1) ν_Q is the quadrupole coupling constant proportional to the largest EFG component, η is the quadrupole asymmetry parameter ($\eta = 0$ for axial symmetry), and $\boldsymbol{K}$ is the Knight shift tensor. The magnetic field necessary to tune each transition at constant frequency is then

0925-8388/93/$6.00

a function of the angles between the magnetic field and the axes of the Knight shift and quadrupole tensors. A powder pattern line shape is the experimental result of combining spectra of crystallites distributed uniformly over all possible orientations.

The line shape obtained in a simulation by perturbation calculation depends on the order of the calculation, the quadrupole constant, the asymmetry parameter and the anisotropic part of the Knight shift. The Zeeman effect and the isotropic part of the Knight shift do not alter the shape, only the position of the resonance. To first order, the powder spectrum of an Al ($I=5/2$) nucleus with $\eta,K=0$ consists of a narrow, central $1/2 \leftrightarrow -1/2$ line with satellites equally distributed on both sides resulting from the $\pm 3/2 \leftrightarrow \pm 1/2$ and $\pm 5/2 \leftrightarrow \pm 3/2$ transitions. The $\pm 3/2 \leftrightarrow \pm 1/2$ transitions give maxima separated from the central line by an amount $\nu_Q/2$ in frequency units, with non-zero amplitude extending to ν_Q on the opposite side of the central line, while the $\pm 5/2 \leftrightarrow \pm 3/2$ lines are distributed twice as widely. In second order the central transition develops additional structure and can display a clear double-peaked powder spectrum. For larger values of η, the peaks of all the transitions tend to merge and become more difficult to resolve. The full width of the central transition can be described as a competition between the second order quadrupole effects and the anisotropic Knight shift K_{aniso} by

$$\Delta\nu = \frac{25\nu^2_Q\{I(I+1)-3/4\}}{144\nu} - \frac{5\nu K_{aniso}}{3} + \frac{\sigma}{2} \qquad (2)$$

where σ is the dipolar contribution to the line width [8]. At low frequencies, the quadrupole effects dominate while for high frequencies, the anisotropic Knight shift will dominate. With spectra taken at several frequencies, eqn. (2) can be used to estimate both K_{aniso} and ν_Q.

The isotropic part of the Knight shift tensor, K_{iso}, provides important information on the density of electronic states near the Fermi level. Conduction-electron–nuclear contact causes a shift of the resonance by an amount proportional to the Pauli spin susceptibility. In the independent electron approximation, this susceptibility is proportional to the electronic density of states at the Fermi level $\rho(E_F)$. For convenience, K_{iso} is usually expressed relative to the resonance of an insulating standard ($\rho(E_F)=0$)

$$K_{iso} = \frac{\Delta H}{H} \cong \frac{H_0 - H_{sample}}{H_0} \propto \rho(E_F) \qquad (3)$$

For aluminum metal $K_{iso} = +0.16\%$ measured with respect to the resonance of insulating $AlCl_3$ [9].

If a nuclear resonance is saturated, the return to equilibrium is through the transfer of energy to the crystal lattice by the conduction-electron–nuclear contact. The characteristic time is the spin-lattice relaxation time, T_1. A simple calculation shows that T_1T is a constant proportional to $\rho(E_F)^{-2}$. For aluminum metal $T_1T = 1.85$ s K [10].

The Korringa relation expresses the connection between K_{iso} and T_1 as

$$K^2_{iso}T_1T = S = \left[\frac{\gamma_e}{\gamma_n}\right]^2 \frac{h}{8\pi^2 k_B} \qquad (4)$$

where γ_e, γ_n are the electronic and nuclear gyromagnetic ratios. Ideally, the Korringa ratio $K^2_{iso}T_1T/S = 1$, but deviations are common. For aluminum metal the Korringa ratio is 1.2 at 77 K [10]. In most cases the Korringa relation can only provide a rough check of the magnitude of K_{iso} and in many cases is unreliable for estimating very small shifts.

3. Experimental details

The sample for this study was produced and characterized by X-rays at CNRS/CEDEX and LURE by Calvayrac *et al.* The details of production and characterization have been reported elsewhere [11] and are not reproduced here except to say that the X-ray spectra conformed to that expected for a perfect quasicrystal with line widths limited only by the spectrometer resolution. This material was produced by quenching the liquid to room temperature and then annealing for several hours at 1023 K. X-ray spectra recorded after annealing showed a substantial narrowing of the line widths over those recorded before annealing. Subsequent anneals did not produce any further improvement in the X-ray spectra.

For NMR the sample was placed in a polyethylene vial in the spectrometer's coil. Glass and Pyrex tubes were found to be unsuitable because of observable sodium and boron NMR. Powder pattern spectra were recorded by spin-echo techniques at 11.10, 17.80 and 46.69 MHz and at several temperatures. Spin-echoes were coherently detected and integrated using a boxcar integrator while the external magnetic field was swept. The resulting spectra are shown in Figs. 1(a)–(c), each with a corresponding simulation (discussed below). The spectra shown for 11.10 and 17.8 MHz were recorded at 77 K and the spectrum for 46.69 MHz was recorded at 50 K.

To determine the Knight shift of the NMR resonance accurately, the field of the resonance peak was measured using a Hall probe placed in close proximity to the sample coil. With the icosahedral sample removed and replaced with a similar amount of powdered aluminum metal, the center of the aluminum metal resonance was located by observing the free-induction decay fol-

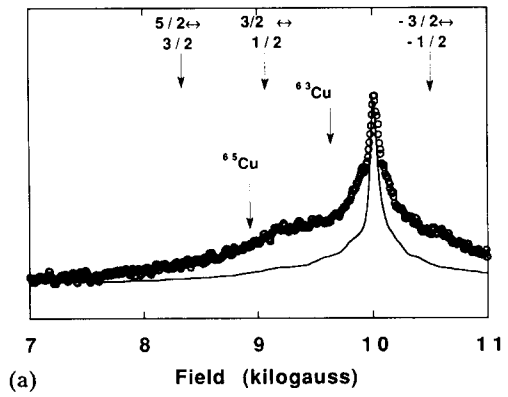

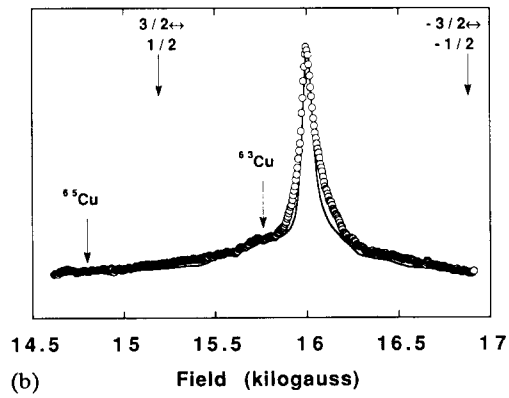

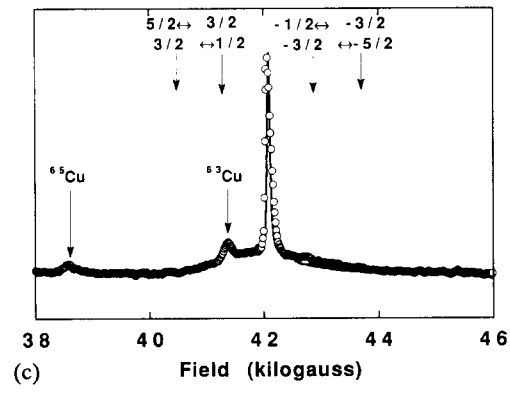

Fig. 1. Experimental (circles) and simulated (curves) NMR spectra of ^{27}Al. Simulations were produced using a quadrupolar asymmetry of $\eta = 0.75$ and a spread of six quadrupole constants from 0.3 to 1.8 MHz. Arrows indicate the positions of the ^{63}Cu and ^{65}Cu resonances and the edges of the ^{27}Al quadrupolar transitions for $\nu_Q = 1.8$ MHz: (a) 11.10 MHz, $T = 77$ K; (b) 17.80 MHz, 77 K; (c) 46.69 MHz, 50 K.

lowing an r.f. pulse and noting the field at which its phase reversed. The Knight shift was then determined from eqn. (3) after correction for the known Knight shift of aluminum metal.

The spin-lattice time T_1 was determined by measuring the amplitude of the spin-echo produced by a 90°–180° pulse sequence delayed from a saturating comb of pulses. An exponential fit to the echo heights as a function of delay time yielded the values of T_1 shown in Table 1. A plot of echo amplitudes *vs.* delay time

TABLE 1. Measured values of T_1 and estimated values of K_{iso} from eqn. (4). The measured value of $K_{iso} = +0.02\% \pm 0.03\%$ and the average value of K_{iso} estimated below is $|K_{iso}| = 0.058\%$

ν (MHz)	T (K)	T_1 (ms)	K_{iso} (%)
11.1	77	165	0.055
11.1	293	42.0	0.056
17.8	293	52.3	0.050
17.8	77	173	0.066
45.36	50	296	0.063
46.69	120	87.7	0.060

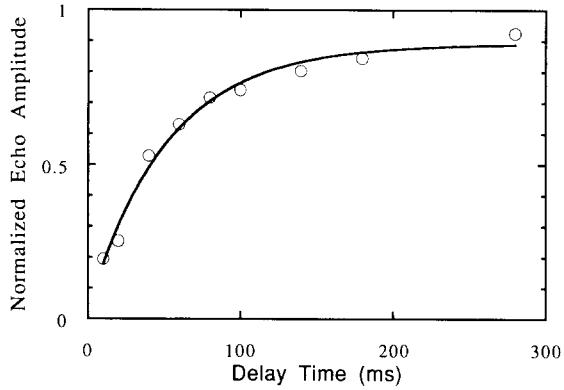

Fig. 2. NMR saturation recovery for $T = 300$ K, $\nu = 17.8$ MHz (circles) fit to an exponential with an additive constant term included to account for imperfect saturation. The fitted value of $T_1 = 52.3$ ms.

with the corresponding exponential fit is shown in Fig. 2 for one frequency and temperature.

4. Results and discussion

The ^{27}Al spectra for AlCuFe display the strong central $+1/2 \leftrightarrow -1/2$ transition together with less prominent wings from the $\pm 1/2 \leftrightarrow \pm 3/2$ and $\pm 3/2 \leftrightarrow \pm 5/2$ transitions. Also visible at lower fields are weaker ^{63}Cu and ^{65}Cu resonances.

The line widths at the three frequencies (full width at half-maximum) were fit using eqn. (2), assuming no intrinsic dipolar line width ($\sigma = 0$) and allowing the parameters K_{aniso} and ν_Q to vary independently. A plot of the line widths is shown in Fig. 3 along with fitting curves showing the relative contributions from the two terms. This analysis sets an upper limit for the anisotropic Knight shift of $K_{aniso} = -0.09\%$. Since this can explain at most about half of the line width at the highest frequency, we have assumed in all simulations that $K_{aniso} = 0$. The value of ν_Q estimated from this analysis is $\nu_Q = 1.35$ MHz. The purely isotropic Knight shift for $Al_{63}Cu_{24.5}Fe_{12.5}$ is small and is not likely to affect the line shape.

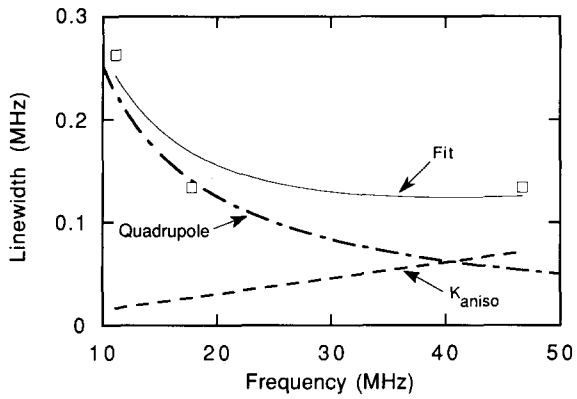

Fig. 3. Measured NMR line widths for three frequencies (squares) and fit (solid curve) to eqn. (2). The fitted values of K_{aniso} and ν_Q are $K_{aniso} = -0.09\%$ and $\nu_Q = 1.35$ MHz. Dashed curves show the relative contributions to the measured linewidths from the quadrupolar and anisotropic Knight shift terms individually.

In order to simulate the observed powder patterns, a computer program adapted by E. J. Friebele from Taylor and Bray's line shape simulation program [12] was utilized. Since it is difficult to accomplish a meaningful least-squares analysis of experimental spectra, it is necessary to make prudent choices of parameters in order to obtain a reasonable simulation of the spectra for all three frequencies. This procedure does not necessarily produce unique solutions and only in the best of circumstances can it be regarded as definitive. In the worst case, there can be many sites with different quadrupole constants, asymmetry parameters and Knight shift parameters simultaneously. Such a scenario is nearly hopeless without a significant contribution from either luck or theoretical direction. The best approach to a complex modelling situation is to use the available evidence to eliminate unlikely contributions to the simulations, and then to start from the simplest scenario possible, adding complexity as needed.

The most obvious features of note in the spectra are the lack of any splitting of the ^{27}Al central peak and the broad, nearly featureless ^{27}Al quadrupole pedestal. The second order quadrupole effect with zero asymmetry causes a splitting of the central peak in powder pattern spectra. This splitting is effectively removed for large values of the asymmetry parameter η. The featureless central peak at all three frequencies (Figs. 1(a)–(c)) thus suggests a large value for the asymmetry parameter. From our simulations we find $\eta = 0.75$ is the minimum value necessary to merge the central peak. An estimate of this parameter from theory is possible, though it would require complex calculations that are presently unavailable. Using the width of the quadrupole pedestal at the highest frequency, ν_Q is estimated to be 1.8 MHz, though this value is somewhat larger that the 1.35 MHz estimated from the line width analysis. The *net* isotropic Knight shift was measured to be very small (discussed in more detail below) and we neglect its effect in our simulations. The anisotropic Knight shift determined from the line-width analysis is also small and is likewise neglected. Rubinstein and Stauss [1] discussed the possibility of multiple sites for the aluminum in AlMnSi. A distribution of sites could contribute as either multiple quadrupole constants, multiple Knight shifts or both. For AlCuFe we note that the spin-lattice relaxation proceeds with a time dependence that is well described by a single exponential in time (discussed in more detail below) and with relaxation times that have the expected $1/T$ dependence. Since the spin-lattice relaxation time and the Knight shift are both determined fundamentally by the electron–nuclear contact, a distribution in Knight shifts would necessarily imply a similar distribution of relaxation times. Such a distribution is not apparent and we therefore exclude the possibility of a distribution of Knight shifts.

Using this information, simulations were initially obtained assuming a single value of ν_Q and a large asymmetry. These early attempts were unacceptable because of the presence of structure in the simulations that is not observed experimentally, and of difficulty in reconciling the width of the quadrupole pedestal with the width of the central transition. More successful were simulations that included some contribution from very small values of ν_Q. The proper amount of both pedestal intensity and central peak intensity was only obtained when the simulations were expanded to include multiple values of ν_Q. The quality of the simulations showed sensitivity to both the extreme values of ν_Q and the relative contribution from "interior" values (quadrupole terms $0.3 < \nu_Q < 1.8$ MHz). Our best simulation of the spectra utilized six discrete values of ν_Q equally spaced from 0.3 MHz to 1.8 MHz, all with equal weight, and each with $\eta = 0.75$. This final simulation includes the contribution from two copper isotopes each with a single value of ν_Q (^{63}Cu: $\nu_Q = 7.35$ MHz, ^{65}Cu: $\nu_Q = 7.95$ MHz) chosen to reproduce the observed heights with allowance for stoichiometric abundances, relative sensitivities, and quadrupole moments. Since satellite structures and central-peak splitting were not observed in the copper resonances, a large asymmetry was also assumed ($\eta = 1.0$). The resulting simulations are shown as the solid traces in Figs. 1(a)–(c). We note good agreement between the simulations and data for the 17.8 and 46.69 MHz spectra, but poor agreement for the 11.1 MHz spectra's quadrupole pedestal, although the 11.1 MHz central peak's full width at half-maximum is approximately reproduced. We were unable to find a set of parameters that simultaneously simulate the central peak widths and the quadrupole pedestals for all three frequencies adequately. Several spectra taken at 11.1 MHz consistently reproduce the

features displayed in Fig. 1(a), and we are unable to offer an explanation for our inability to model all three spectra simultaneously.

To test the possibility that a better description of the distribution of aluminum sites is a continuous spread of values of ν_Q from 0.3 MHz to 1.8 MHz, we "filled in" the set of six discrete values of ν_Q with contributions from 10 additional sites, resulting in a set of 16 quadrupole terms equally weighted and equally spaced from 0.3 to 1.8 MHz. The resulting simulations were judged to be unacceptable because of a significant excess of intensity near the central peak. We conclude that a continuous rectangular distribution of quadrupole terms over the range described is inappropriate. We cannot exclude the possibility that a more complex distribution of discrete or continuously varying sites would give better results although, without more justification, any attempts at further refinements would be unnecessarily speculative.

We note that the NMR spectra of AlMnSi [1], and AlMnSiRu [2] also show structureless resonance peaks and smooth quadrupole pedestals. Fujimaki *et al.* [2] see clear evidence for magnetic broadening of the resonance line of AlMnSiRu at low temperatures, though the line widths they observe at all temperatures are significantly larger than those seen for AlMnSi or AlCuFe. Line shapes for AlCuFe at 17.8 MHz show no broadening at 77 K relative to the room temperature spectrum (not shown), indicating that there is no magnetic broadening at 77 K.

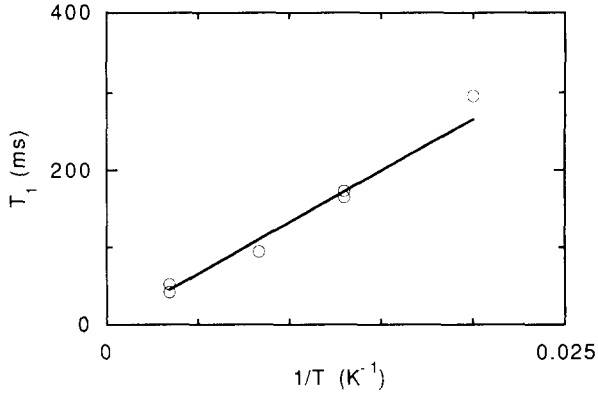

Fig. 4. ^{27}Al NMR relaxation data *vs.* inverse temperature fit with simple power-law expression $T_1 = \text{const.}(1/T)^n$ where the fitted value of n is 1.006 and the proportionality constant is 13.63 sK.

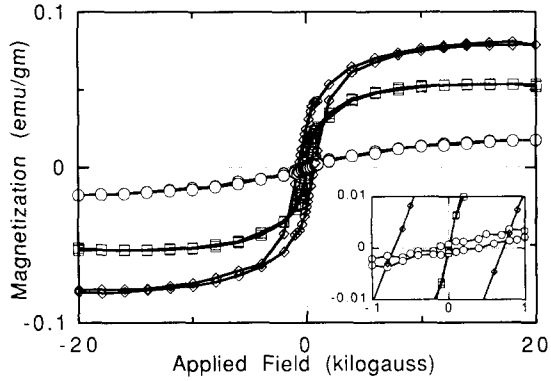

Fig. 5. Magnetization loops for AlCuFe at 295 K (circles), 100 K (squares) and 5 K (diamonds). The inset graph show an expanded view of the region near zero field.

5. Knight shifts and spin-lattice relaxation

In $Al_{63}Cu_{24.5}Fe_{12.5}$ the isotropic Knight shift is found to be very small ($K_{iso} = +0.02\% \pm 0.03\%$) when compared with the insulating standard $AlCl_3$. This small value of K_{iso} is consistent with other NMR results for AlMnSi [1], AlMnSiRu [2] and AlCuLi [3] and also consistent with the proposed pseudo-gap in the electronic density of states at the Fermi level.

Measurements of the spin-lattice relaxation time T_1 were performed at several frequencies and temperatures. The spin-echo intensity measured as a function of delay time following a saturating comb of pulses is shown for one temperature and frequency in Fig. 2 together with a fit to an exponential recovery form. The fit includes a constant offset term to account for imperfect saturation. Recovery was in all cases found to be well described by an exponential. A plot of the values of T_1 *vs.* inverse temperature in Fig. 4 shows the expected linear dependence. Since T_1T is inversely proportional to $\rho^2(E_F)$, it is worthwhile to compare the value for aluminum metal ($T_1T = 1.8$ s K) and AlCuFe ($T_1T = 13.63$ s K). This result is clearly consistent with a weak density of states at the Fermi level for AlCuFe.

Estimating the Knight shift from the Korringa relation (eqn. (4)) yields an average value of $|K_{iso}| = 0.058\%$. Table 1 shows the results of measurements of T_1 and the estimated magnitude of K_{iso} from eqn. (4). Although the estimates of K_{iso} are not in precise agreement with the measured Knight shift of $+0.02\% \pm 0.03\%$, they are on average only one third of the value for pure aluminum metal. The qualitative agreement of the Korringa relation with the measured Knight shift implies that the small Knight shift is due almost entirely to a low density of states at the Fermi level and not to a cancellation of terms from s–p hybridization [1].

6. Magnetization and Mössbauer

Magnetization curves taken at 295, 100 and 5 K are shown in Fig. 5. These curves are representative of a ferro- or ferrimagnetic phase. Very little hysteresis is observed in the 295 and 100 K loops, but significant hysteresis is evident for the 5 K loop. If this magnetic

behavior is ascribed to an impurity phase then we can estimate the fraction of iron atoms contributing to the magnetism by assuming only iron atoms with a moment of $2\mu_B$ contribute. If these moments are fully aligned at 5 K and 20 kG, at most 0.3% of the iron atoms could be in this phase. In contrast, if the magnetism is not due to an impurity phase and all iron atoms in the alloy carried and equal moment, only $0.01\mu_B$ per iron would be needed to account for the observed magnetism. Such a small moment is unlikely in our view. Since NMR spectra show no magnetic broadening at low temperatures we conclude that the observed magnetism is due to a small amount of a magnetic impurity phase and not due to the icosahedral phase itself.

Mössbauer spectra taken at room temperature and 4.2 K are shown in Fig. 6. These spectra are similar to those previously reported for Al–Mn quasicrystals containing small fractions of iron substituted on the Mn site [13]. The line-shapes are closely fitted using lorentzian lines with the parameters shown in Table 2. Fits to the two lines indicate an average quadrupole splitting of 0.394 mm s^{-1} at room temperature and 0.407 mm s^{-1} at 4.2 K, with a small amount of additional broadening of the 4.2 K lines relative to the room temperature spectrum. A magnetic moment at each iron site ordering at low temperatures should cause large broadening of the 4.2 K lines relative to the room temperature spectrum. We interpret the lack of such an effect as indicative of magnetism in a separate impurity phase. If magnetic interactions are discounted as a broadening mechanism then the observed splitting in the spectra must arise from a distribution of quadrupole-split lines. Improved fits are obtained with two or more quadrupole splittings. In particular, the spectra of Fig. 6 are well fit for a distribution of six equally spaced lines with nearly equal intensities and linewidths of 0.23 mm s^{-1} and splitting between 0.17 and 0.59 mm s^{-1}. Although no direct comparison between the iron site and the aluminum site is possible, the Mössbauer measurements are consistent with a similar distribution of local environments for the two nuclei. The asymmetry of the spectra can be accounted for by ascribing a slightly different isomer shift to each quadrupole. Isomer shifts between 0.220 and 0.225 mm s^{-1} reproduced the observed asymmetry.

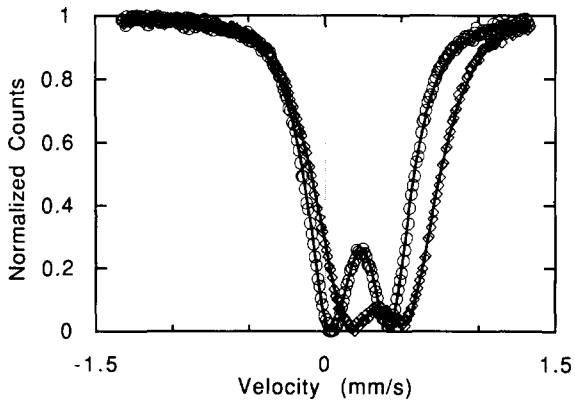

Fig. 6. Mössbauer effect spectra at 295 K (circles) and 4.2 K (diamonds) with fits to single line Mössbauer effect functions (curves).

TABLE 2. Fitting parameters for the Mössbauer spectra using a single quadrupole splitting for each line. Line positions are relative to pure iron at room temperature

Line	T (K)	Intensity	Width (mm s^{-1})	Position (mm s^{-1})
1	295	0.52	0.52	0.006
2	295	0.48	0.42	0.400
1	4.2	0.52	0.56	0.138
2	4.2	0.48	0.49	0.545

7. Conclusions

A pseudo-gap has been suggested by band-structure calculations [7, 14, 15] and electronic transport measurements [4–6] in a multitude of icosahedral materials and has been proposed as a universal feature of this class of materials [15]. These calculations imply that the existence of a pseudo-gap is the result of localization of conduction electrons and that this facilitates the formation of the icosahedral phase [7, 14, 15]. Our NMR measurements confirm the existence of such a feature in icosahedral AlCuFe, and place it squarely in agreement with previous results for AlMnSi [1], AlMnSiRu [2] and AlCuLi [3]. Furthermore, the thermodynamic stability of AlCuFe lends strong support to the results from earlier measurements in alloys that were not thermodynamically stable.

We find the ^{27}Al NMR line shapes in AlCuFe are best explained in terms of a distribution of electric field gradients with large asymmetry. Magnetization measurements indicate the presence of a small amount of ferro- or ferrimagnetism, and Mössbauer spectra show a small broadening at 4.2 K relative to the room temperature spectrum. Based on the results from the magnetism and Mössbauer spectra, we conclude that the observed magnetism is due to a second minority phase and does not affect the NMR line shapes. The Mössbauer effect spectra also are characteristic of a distribution of quadrupole splitting of the iron nuclei. Although no direct quantitative comparison between the aluminum site NMR and the iron site Mössbauer is possible, we find the qualitative similarity of a distribution of local environments at the two nuclei reassuring.

Acknowledgments

We wish to thank D. Gratias for the sample provided and J. Cahn, and B. Mozer for their helpful comments. J. Friebele's powder pattern simulation program has been an integral part of our research and we gratefully acknowledge his assistance. Finally, we wish to thank the Office of Naval Technology for its support of A. Drews through a postdoctoral fellowship.

References

1 M. Rubinstein and G. H. Stauss, *J. Mater. Res., 1*(2) (1986) 243–246.
2 H. Fujimaki, K. Motoya, H. Yasuoka, K. Kimura, T. Shibuya and S. Takeuchi, *Technical Report of ISSP,* The University of Tokyo, Series A, No. 2388, 1991.
3 C. Lee, D. White, B. H. Suits, P. A. Bancel and P. A. Heiney, *Phys. Rev. B., 37* (1988).
4 B. D. Biggs, S. J. Poon and N. R. Munirathnam, *Phys. Rev. Lett., 65*(21) (1990) 2700.
5 T. Klein, C. Berger, D. Mayou and F. Cyrot-Lackmann, *Phys. Rev. Lett., 66*(22) (1991) 2907.
6 K. Kimura and S. Takeuchi, *Technical Report of ISSP,* Series A, No. 2379, 1991.
7 T. Fujiwara and T. Yokakawa, *Phys. Rev. Lett., 66*(3) (1991) 333.
8 R. G. Barnes, F. Borsa, S. L. Segel and D. R. Torgeson, *Phys. Rev., 137*(6A) (1965) A1828.
9 E. R. Andrew, W. S. Hinshaw and R. S. Tiffen, *Phys. Lett., 46A*(1) (1973) 57.
10 J. J. Spokas and C. P. Slichter, *Phys. Rev., 113*(6) (1959) 1462.
11 Y. Calvayrac, A. M. Bessiere, S. Lefebvre, M. Cornier-Quiguandon and D. Gratias, *J. Phys. Paris, 51* (1990) 417–431.
12 E. J. Friebele, *NMRLINE Computer Program,* Naval Research Laboratory, Washington, DC 20375, unpublished, adapted from P. C. Taylor and P. J. Bray, *Line-Shape Program Manual,* Physics Department, Brown University, Providence, RI 02912, 1968, unpublished.
P. C. Taylor and P. J. Bray, *J. Magn. Res., 2*(3) (1970) 305.
13 L. J. Swartzendruber, D. Schectman, L. Bendersky and J. W. Cahn, *Phys. Rev. B* (1985) 1383.
14 V. G. Vaks, V. V. Kamyshenko and G. D. Samolyuk, *Phys. Lett. A, 132*(2, 3) (1988) 131.
15 T. Fujiwara, *Phys. Rev. B, 40*(2) (1989) 942.